INTERNATIONAL ATOMIC ENERGY AGENCY
UNITED NATIONS EDUCATIONAL, SCIENTIFIC AND CULTURAL ORGANIZATION

INTERNATIONAL CENTRE FOR THEORETICAL PHYSICS
34100 TRIESTE (ITALY) - P.O.B. 586 - MIRAMARE - STRADA COSTIERA 11 - TELEPHONE: 2240-1
CABLE: CENTRATOM - TELEX 460392-I

SMR/208 - 34

SPRING COLLEGE IN MATERIALS SCIENCE

ON

"METALLIC MATERIALS"

(11 May - 19 June 1987)

POSITRON STUDIES ON DEFECTS AND MECHANICAL PROPERTIES OF METALS

C.W. LUNG
Institute of Metal Research
Academia Sinica
Wenhua Road
Shenyang
People's Republic of China

POSITRON STUDIES on DEFECTS and MECHANICAL PROPERTIES of METALS

I. Introduction to PA

Special advantages:

Sensitive to the presence of defects.

$\sim 10^{-7}$ vacancy concentration

For studies of nondilute alloys

$> 1\% \rightarrow 100\%$

For studies under wide range temperatures

Wide range of fields

metals, semiconductors, ionic solids, polymers....

mechanical engineering, materials science,

solid state physics, theoretical physics...

Not very expensive

~ US $ 20,000 - 40,000.

References

1. P. Hautojärvi, [illegible]

Springer, Berlin, [illegible].

2. W. Brandt and A. Dupasquier,

[illegible] Solid State Physics, Proc. Inter.

Sch. Phys. "Enrico Fermi", North-Holland

Publ. Co. (1983).

3. P. C. Jain, R. M. Singru and K. P. Gopinathan,

Positron Annihilation, Proc. ICPA-7.

World Scientific, (1985).

4. C. W. Ling and N. H. March, Cryst. Latt.

Def. and Amorph. Materials. 13 (1986) 31.

I. 1. Thermalization

e^+ Source: ^{22}Na (0.54 Mev), ^{64}Cu (0.65), ^{57}Co (0.48), ^{68}Ge (1.4) γ-ray (1.28 Mev)

time: $\sim 10^{-12}$ sec.

distance: 10 – 1000 μm.

energy: $kT(\sim 30^\circ C) \sim 0.025$ eV.

2. Annihilation: ($\gamma \ll \alpha = \frac{1}{137}$)

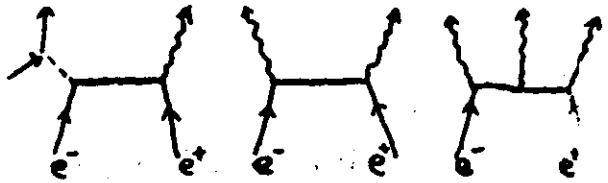

$\sigma_{(2)}/\sigma_{(3)} \approx \alpha$. $\sigma_{(1)}/\sigma_{(2)} \approx \alpha^0$

$\sigma_{(2)} = \frac{\pi r_0^2 c}{v}$

$\Gamma_{(2)} = \sigma_{(2)} v n_e = \pi r_0^2 c n_e$

$2 m_0 c^2 = 2 \times 0.511 \times 10^6$ eV γ

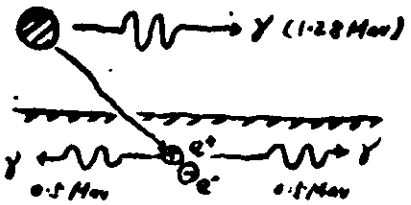

II. Lifetime $\tau = \Gamma^{-1}$

	Solid	Liquid	Gas
τ (sec)	$\sim 10^{-10}$	$\sim 10^{-9}$	$\sim 10^{-7}$

$\tau_p < \tau_d$

III. Angular correlation

e^-, e^+ static: $\vec{P}_1 + \vec{P}_2 = 0$; $\vec{c}_1 = -\vec{c}_2$; 180°

e^- motion: $\vec{P}_1 + \vec{P}_2 \neq 0$ $\vec{c}_1 \neq -\vec{c}_2$; θ_{12}

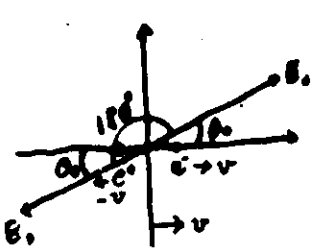

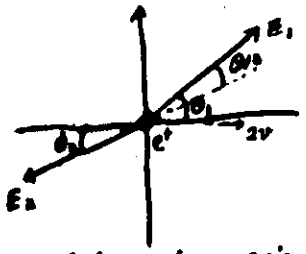

(a) Axis system of center of mass (b) Laboratory axis system

$\sum P_i = m(v_1 + v_2) = m(-v + v) = 0$

$\theta_{12} \cong \theta_1 - \theta_2 \cong \frac{\frac{v}{c}\sin\theta_0}{1 - \frac{v}{c}\cos\theta_0} = \frac{\frac{v}{c}\sin\theta_0}{\frac{P_z}{m_0 c}}$

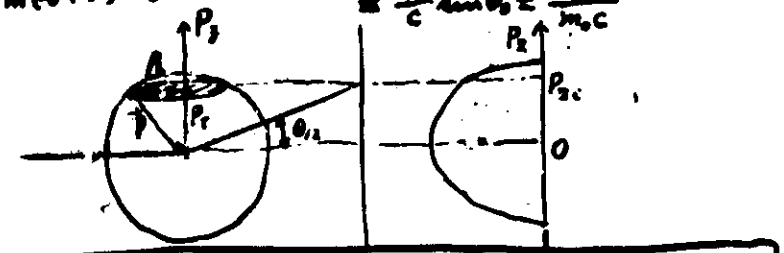

$$N(\theta_2) = C \int_{-\infty}^{+\infty} \int_{-\infty}^{\infty} dp_x\, dp_y\, \Gamma(p_x, p_y, \theta_2, m_0 c) = N(p_z)$$

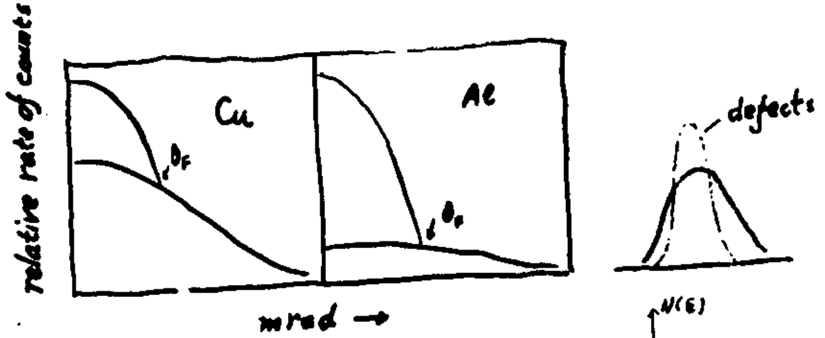

IV. Doppler broadening

$$E_{1,2} \approx \frac{1}{2} E_T' \left(1 \pm \frac{v}{c} \cos\theta_0\right)$$

$$\approx m_0 c^2 \pm \frac{c P_L}{2} = E_0 \pm \delta E$$

$$P_L = 2 m_0 v \cos\theta$$

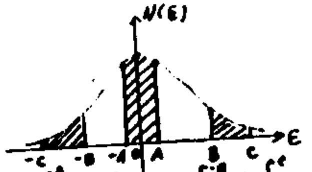

$$H = \frac{\int_{-A}^{A} N(E)\,dE}{\int_{-\infty}^{\infty} N(E)\,dE}, \quad W = \frac{\int_{-C}^{-B} + \int_{B}^{C}}{\int_{-\infty}^{\infty} N(E)\,dE}$$

$$S = \frac{H}{W}, \quad D = H - W, \quad R = \left|\frac{H - H_f}{W - W_f}\right|$$

V. Interaction between e^+ and vacancy

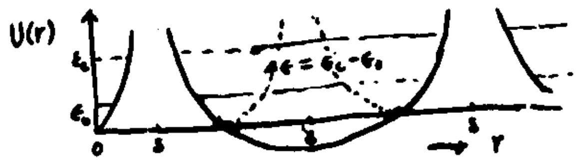

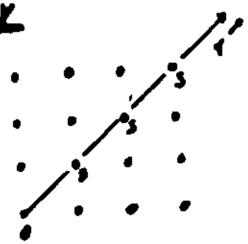

VI. trapping model

$$\frac{dn_f(t)}{dt} = -\left(\frac{1}{\tau_f} + \sum_{j=1}^{m} \sigma_j(t) C_j\right) n_f(t) + \sum_{j=1}^{m} \nu_j n_j(t)$$

$$\frac{dn_j(t)}{dt} = -\frac{n_j(t)}{\tau_j} + \sigma_j(t) C_j n_f(t) - \nu_j n_j(t)$$

$$(j = 1, 2, \cdots, m)$$

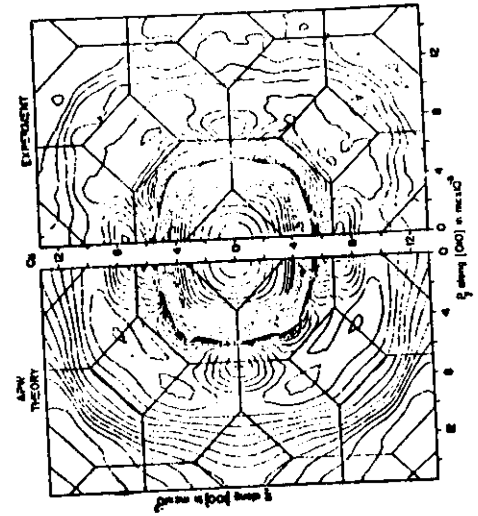

Fig. 9 Contour maps of experimental vs theoretical $K(p_y,p_z) - \bar{K}(p_y,p_z)$ for Cu with p_x along the [001] direction. $\bar{K}(p_y,p_z)$ is a smooth rotationally symmetric surface as discussed in the text, and is used to exhibit the anisotropies at high momenta. The steps of the contour lines are changed at around p~3.5 mrad as discussed in the text.

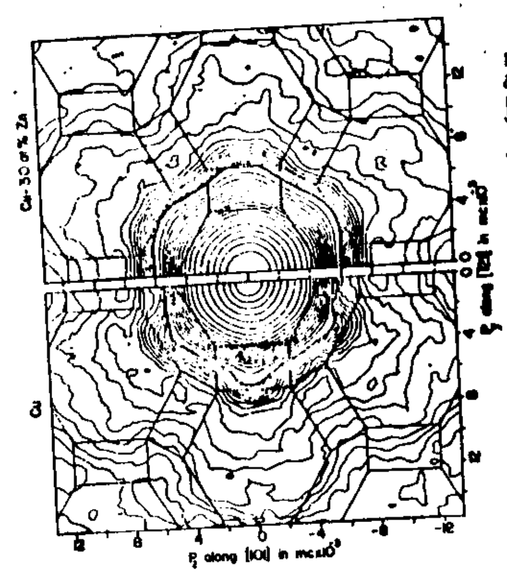

Fig. 13 The contour map of the $K(p_y,p_z) - \bar{K}(p_y,p_z)$ surfaces from Cu vs Cu-30 at.% Zn, orientated with p_x along the [111] direction. $\bar{K}(p_y,p_z)$ is a smooth rotationally symmetric surface as discussed in the text, used to exhibit the anisotropies at high momenta.

We have applied our 2D technique to the study of α-brass. Full 2D ACAR surfaces have been measured for Cu-11.6 at.% Zn [94] and Cu-30 at.% Zn, [illegible]

Assuming: $\gamma_j = 0$ (no detrapping) A. Sugar (J. Phys. F. 3 (1973) 248)

$\sigma_j(t) = \sigma_j$

The solution is

$$n_f(t) = n_f(0) \exp(-t/\tau_0)$$

$$\left(\frac{1}{\tau_0} = \frac{1}{\tau_f} + \sum_{j=1}^{m} \sigma_j c_j\right)$$

$$n_j(t) = \tau_0 \tau_j \frac{\sigma_j c_j}{\tau_0 - \tau_j} n_f(0) \exp(-t/\tau_0) + \left[n_j(0) - \tau_0 \tau_j \frac{\sigma_j c_j}{\tau_0 - \tau_j} n_f(0)\right] \exp(-t/\tau_j)$$

$j = 1, 2, \cdots m.$

For spherical attractive potential wells, one obtains

$$\sigma_j(t) = \frac{4\pi r_j D}{\Omega}\left[1 + r_j (\pi D t)^{-\frac{1}{2}}\right]$$ Waite's theory

or $$\sigma_j(t) \approx \frac{4\pi r_j D}{\Omega}$$

where Ω is the atomic volume, and D the diffusion coefficient.

$$k = \left\{ \begin{matrix} \sigma \\ \mu \end{matrix} \right\} C_t$$

k: trapping rate; σ, μ: specific ~; C_t: concentration of traps of type j

$$\bar{\tau} = \frac{\int_0^\infty [n_f(t) + \sum_{j=1}^{m} n_j(t)]\, dt}{n_f(0) + \sum_{j=1}^{m} n_j(0)}$$

$$\bar{\tau} = \tau_f \cdot \frac{1 + \sigma \tau_e C_{iv}}{1 + \sigma \tau_f C_{iv}}$$ (for monovacancy)

or: $$\frac{\bar{\tau} - \tau_f}{\tau_e - \tau_f} = \frac{\sigma C_{iv}}{\alpha + C_{iv}\sigma};$$ $$\boxed{\frac{\bar{\tau} - \tau_f}{\tau_e - \bar{\tau}} = \tau_f \sigma_i C_{iv}}$$

$$\sigma = \frac{4\pi D r_{iv}}{\Omega}$$

$$\bar{\tau} = \tau_f \cdot \frac{1 + (4\pi r_{iv} e_{iv} \tau_{iv} D/\Omega)}{1 + (4\pi r_{iv} C_{iv} \tau_f D/\Omega)}$$

$$C_{iv} = \exp(S_{iv}^f/k) \exp(-H_{iv}^f/kT)$$

$$\boxed{H_{iv}^f = kT\left[\frac{S_{iv}^f}{k} + \ln\left(\frac{4\pi D}{\Omega} r_{iv} \tau_f\right) + \ln\left(\frac{\tau_{ik} - \bar{\tau}}{\bar{\tau} - \tau_f}\right)\right]}$$

(vacancy formation energy)

VII. $$\Gamma_e = \pi r_e^2 c\, n_e$$

$$\Gamma_e(p) = (\pi r_e^2 c) \frac{1}{(2\pi)^3} \sum_i \left| \int d\underline{r}\, \exp(-i\underline{p}\cdot\underline{r}) \psi_e(\underline{r}) \psi_+^*(\underline{r}) \right|^2$$

$\psi(\vec{r})$: electron wave function

$\psi_+(\vec{r})$: positron wave function

$r_e = e^2/mc^2$: the classical electron radius.

VIII. e^+ and defects — pseudopotential and pseudo wave function

$H\psi_k(\vec{r}) = E_0\psi_+(\vec{r})$

1. $\psi_k(r) = U(r-R)\,\varphi_k(r)$ (perfect crystal)

$$\left[-\frac{\hbar^2}{2m}\frac{\partial^2}{\partial r^2} + V_a(r)\right]U(r) = E_{ws}\,U(r)$$

$$\left.\frac{\partial U}{\partial r}\right|_{r=R_0} = 0 \qquad R_0: \text{muffin-tin radius}$$

$$\left[-\frac{\hbar^2}{2m}\nabla^2 + w(r)\right]\varphi_k(r) = E_0(k)\,\varphi_k(r)$$

where,

$$w(r) = \begin{cases} E_{ws} + V(r) - V_a(r-R) - \dfrac{\hbar^2}{m}\dfrac{\nabla U(r)}{U(r)}\cdot\nabla & (\text{in}) \quad (w<v) \\ V(r) & (\text{between}) \end{cases}$$

2. defect crystal

$$V(r) = \sum_i V_{ref}(r-R_i) + \Delta V(r) + V_{corr}(r)$$

$$V_{ref}(r) = \begin{cases} V_{ai}(r), & (\text{in}) \\ 0, & (\text{outside}) \end{cases}$$

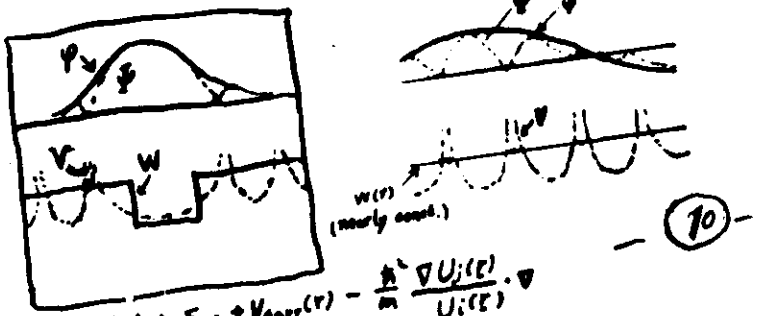

$$w(r) = \Delta V(r) + E_{ref} + V_{corr}(r) - \frac{\hbar^2}{m}\frac{\nabla U_i(r)}{U_i(r)}\cdot\nabla$$

IX. Annihilation characteristic

1-D angular correlation curve

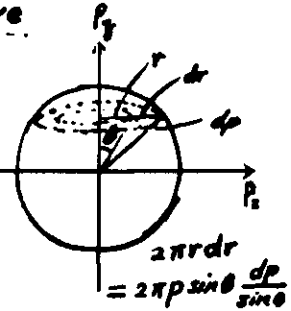

$$I(p_z) = \int dp_x \int dp_y\, \Gamma_0(p)$$

isotropic: e^+-e^- overlaping integral

$$I(p_z) = 2\pi\int_{p_z}^{\infty} dp\cdot p\;\Gamma_0(p)$$

homogeneous electron gas: $\Gamma_0(p) = \frac{\pi r_0^2 c}{(2\pi)^3}$

$$\boxed{I(p_z) = \frac{r_0^2 c}{4\pi}\left(p_F^2 - p_z^2\right)\theta(p_F - |p_z|)}$$

($|p_z| < p_F$ 일 때, $\theta(p_z)=1$; $|p_z| > p_F$ 일 때, $\theta(p_z)=0$)

inhomogeneous electron system.

$$\boxed{I(p_z) = \frac{\pi r_0^2 c}{4\pi}\int dr\,|\psi(r)|^2\,\lambda[n(r)].}$$

where, $\lambda[n(r)] = \overset{n(r)}{\underset{\lambda}{=}}\left[p_F(r)^2 - p_z^2\right]\theta\left(p_F(r)^2 - |p_z|^2\right)$

PA studies on Defects and Mechanical Properties of Metals

Positrons tend to locate in low ion density

or in low electron density regions

[illegible] Solid State Phys. and Amorph. Mater.

[illegible] (1976) 31-63

Positron - vacancy interactions

Binding energy $E_b = \Delta E = E_e - E_0$

The Schrödinger equation for the trapped e^+ is

$$H\psi_+(r) + E_b \psi_+(r) = 0$$

E_b: the energy of the trapped positron in a perfect solid

minus the energy of the trapped positron.

$$H = -\frac{\hbar^2}{2m}\nabla^2 + V_e$$

$$V_e = -[\text{illegible}]\,n(r) + V_c(r) + V_{xc}(r)$$

electrostatic (TF) ion density

Hodges C.H. (1970),

E_b = 3.81 eV 2.54 eV (r = 2 a.u.)

Mannien et al. (1975)

Comparison between V_c and TF methods

Metal	E_b	
	V_c	TF
Li	0.00	0.04
Na	0.02	0.19
K	0.02	0.26
Cs	0.01	0.26
Be	0.80	1.32
Mg	0.51	1.04
Al	1.75	2.61
Tl	1.72	2.52
Sn	2.64	3.59

Gupta and Siegel (1977, 1980)

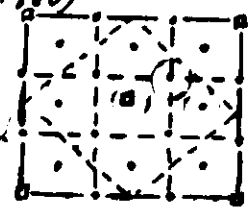

• Al

□ Vacancy

◯ muffin tin potential

Supercell lattice method

APW method

$E_b(Al) = 3.36$ ev

Vacancy cluster

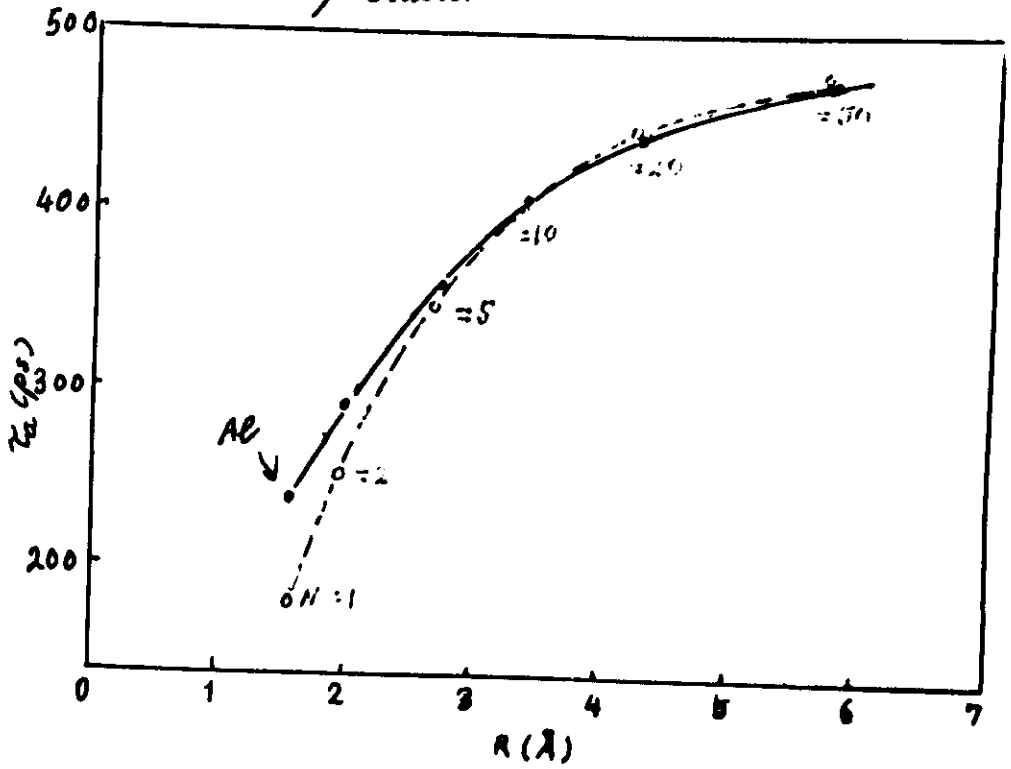

-•- P. Hautojärvi et al. (1977)

•·· [illegible] et al. (1977)

H.E. Hansen et al. J. Phys. F. 14 (1984) 1499

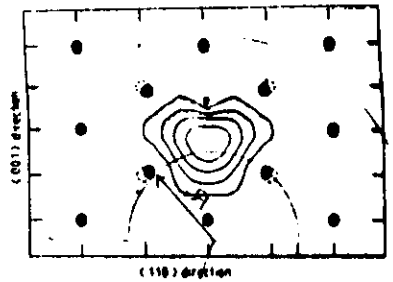

— 14' —

Figure 2. Wavefunction of a positron trapped in a N-decorated Mo vacancy. Full circles indicate Mo ions (note the −7% relaxation of the nearest neighbours to the vacancy). The N atom is indicated by a small open circle.

between the fact that the calculated binding energy of the clean vacancy is twice that of the N-decorated vacancy and the experimental results that the positron trapping rates into these two defects differ little (Nielsen *et al* 1983). For trapping mediated by electron–hole pairs the trapping rate scales linearly with the binding energy if the conduction electrons are treated as plane waves in both initial and final states (Nieminen and Laakkonen 1979). However, one might also argue that introducing the impurity into the vacancy does not necessarily decrease the trapping rate even if it does so for the binding energy: the trapping rate is proportional to the *local* density of final electron states, which may be enhanced by the impurity.

3.3. Hydrogen-decorated vacancies

Hydrogen interactions with lattice defects in metals attract widespread attention (Picraux 1981), partly because of their technological significance. Currently, positron lifetime spectrometry is being introduced into this field with the objective of gaining new detailed information at the atomic level. We expect our model calculations to aid the progress of this work.

Unlike its group V neighbours in the Periodic Table, Mo has a large positive enthalpy of solution for H ($\Delta H_{Mo} \simeq 0.5$ eV, $\Delta H_{Nb} \simeq -0.3$ eV (Völkl and Alefeld 1978)) implying a H solubility 14 orders of magnitude smaller than in Nb at room temperature. Therefore even a small concentration of defects capable of trapping H may increase considerably the solubility of H in Mo just as in the case of N (Anttila and Hirvonen 1978, Nielsen *et al* 1982, Hansen *et al* 1982). Such defects (dislocations, vacancies, voids) may also decrease the H diffusion and thus be responsible for the rather large differences between the reported migration energies of H in Mo (Völkl and Alefeld 1978).

Recent experiments by Nielsen and co-workers (to be published), have clearly demonstrated the potential of the positron lifetime technique for investigation of H interactions with defects in Mo. In the case of vacancies the response is fairly small: the long lifetime in electron-irradiated Mo decreases from 180 to 164 ps after electrolytic injection of H.

Again we shall ask whether this lifetime should be attributed to vacancies decorated by

Vacancy studies with PA

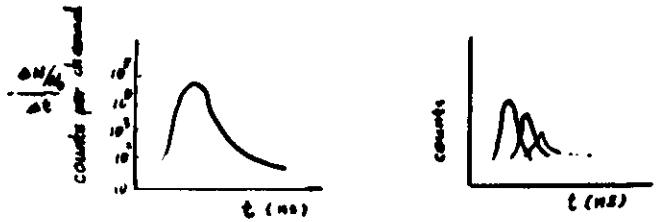

The resulting experimental time spectrum $S(t)$ can be written as the sum of n components

$$S(t) = \sum_{i=1}^{n} I_i \Gamma_i e^{-\Gamma_i t}$$

For simplicity, we discuss the two state trapping model.

$$S(t) = I_1 \Gamma_1 e^{-\Gamma_1 t} + I_2 \Gamma_2 e^{-\Gamma_2 t}$$

$$\Gamma_1 = \lambda_f + k = \tau_1^{-1} \qquad I_1 = \frac{\lambda_f - \lambda_t}{\Gamma_1 - \lambda_t}$$

$$\Gamma_2 = \lambda_t = \tau_2^{-1} \qquad I_2 = \frac{k}{\Gamma_1 - \lambda_t}$$

$$(\lambda_f = \tau_f^{-1}, \quad \lambda_t = \tau_t^{-1}, \quad k = \sigma C_t)$$

$$\sigma C_t = I_2 \left(\frac{1}{\tau_1} - \frac{1}{\tau_2} \right)$$

$$C_t = \exp(S_{iv}^F / k_B) \exp(-H_{iv}^F / k_B T)$$

$$\sigma C_t = I_2 (\tau_1^{-1} - \tau_2^{-1})$$

$$C_t \cong C_{iv} = \exp(S_{iv}^F / k_B) \exp(-H_{iv}^F / k_B T)$$

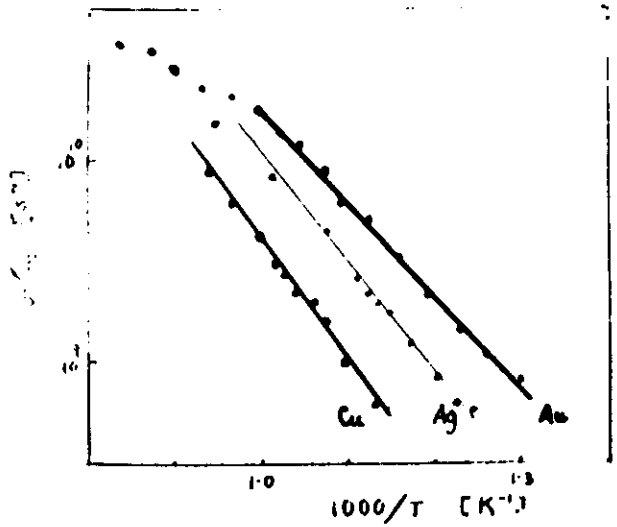

Fig. Arrhenius plots of the trapping rates σC_t with T^{-1} Proc. ICPA-7 (1980) 915 Stuck and Schaefer

Table: Vacancy formation enthalpies H_{iv}^F by PA

Metal	H_{iv}^F (ev)	Metal	H_{iv}^F (ev)
Mg	0·85 ± 0·10	Ta	2·8 ± 0·6
Al	0·68 ± 0·04	Cr	2·0 ± 0·2
In	0·55 ± 0·03	Mo	3·0 ± 0·2
Cu	1·29 ± 0·07	W	4·0 ± 0·3
Ag	1·12 ± 0·07	α-Fe	1·6 ± 0·15
Au	0·89 ± 0·04	Co	1·34 ± 0·07
Zn	0·82 ± 0·07	Ni	1·78 ± 0·10
Cd	0·52 ± 0·02	Pd	1·25 ± 0·25
Pb	0·57 ± 0·06	Pt	1·32 ± 0·04
V	2·1 ± 0·20	Sn	0·50 ± 0·01
Nb	2·65 ± 0·40	U	≈ 1·0

Proc. ICPA-7 (1981) 448 Schaefer

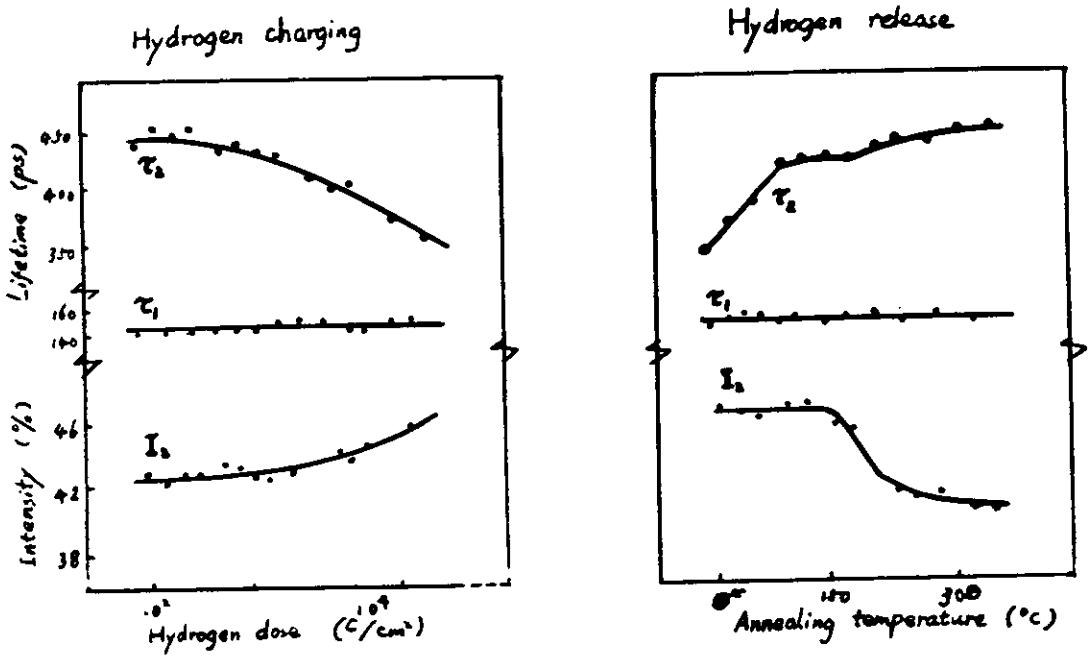

Mo 60°c impl. $1.72 \cdot 10^{18}$ H/cm² annealed up to 450°~650°c ($p < 10^{-7}$ pa)

H: injected electrolytically in 1% H_2SO_4 solution

Fig. Positron lifetime parameters in Mo containing voids (T_{prep} = 450°c) during electrolytical H injection (uncal. scale) and thermal H release.

Proc. ICPA-7 (1985) 497

B. Nielsen et al.

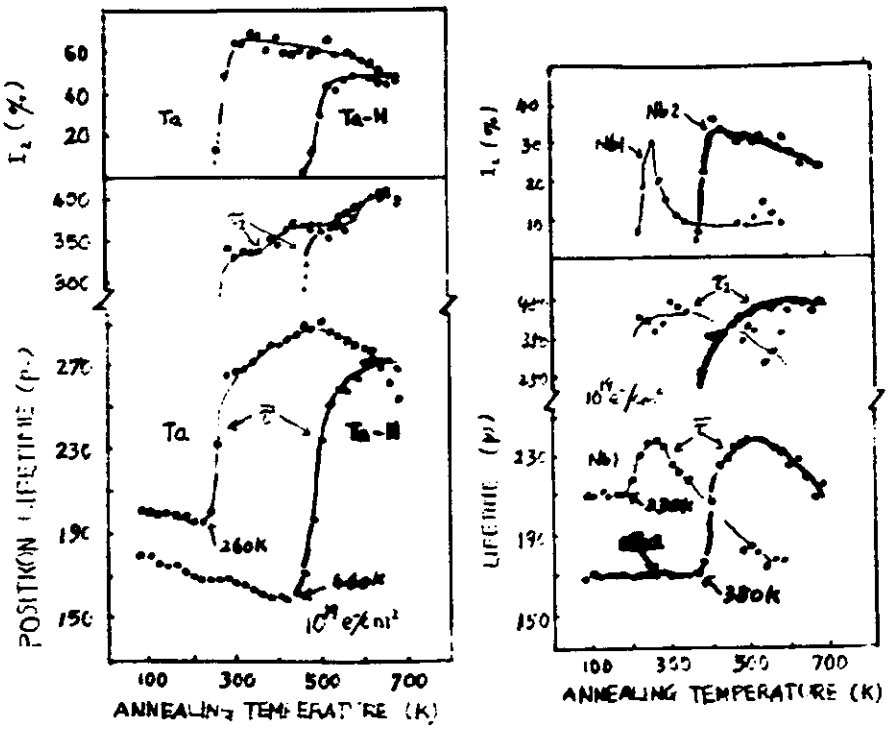

Ta: UHV degassed foil; in H gas at 500K slowly cooling to room temp. H: 1 at%

Proc. ICPA-7 (1985) 519

P. Hautojärvi et al.

Nb annealed at 950°C in HV for 2 hrs before exp.

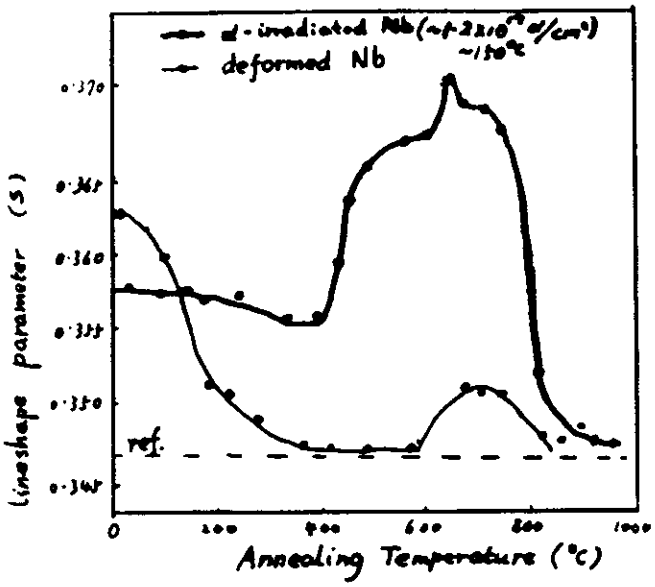

Fig. S – T curve in α-irradiated and deformed Nb (99·8% pure)

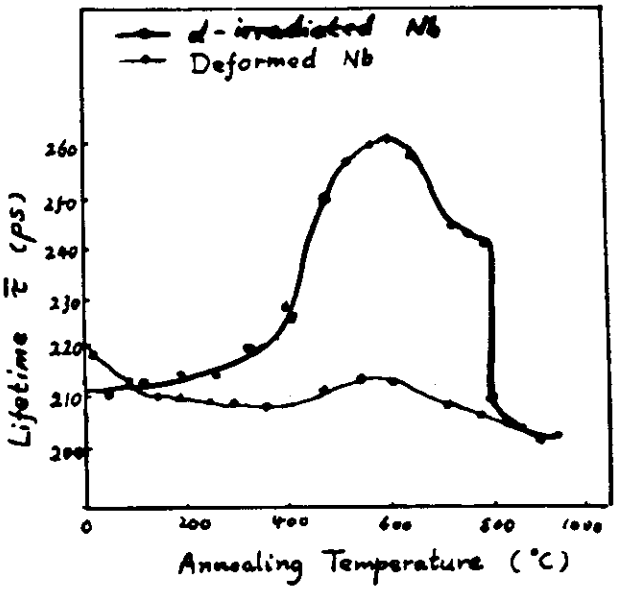

Fig. τ̄ – T in α-irradiated and deformed Nb

Proc. ICPA-7, (1983), 501.
S.V. Naidu et al.

The position of the atom of the impurity atom-
decorated vacancy can be determined by
combination of theoretical calculation and
PA lifetime measurements.

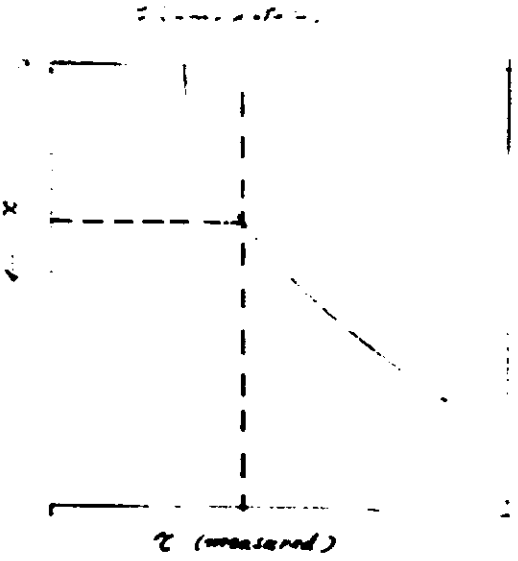

DISLOCATION TRAPS

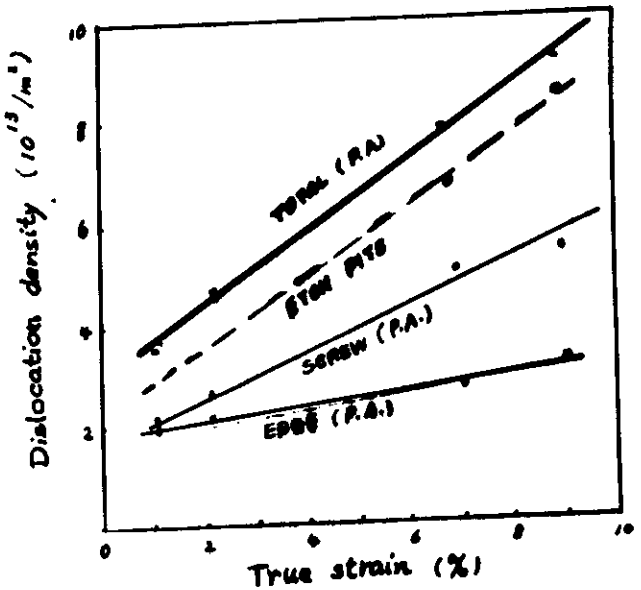

Fig. Dislocation densities measured by PA and etch pits in iron single crystals in tension at 200K.

τ_s = 148 ± 8 ps.

τ_d = 168 ± 5 ps.

$\varepsilon < 10\%$ $\qquad \sigma = K_2/C_2 \approx (1\text{–}10)\times 10^{-2}$ m/s

τ_f = 114 psec

jog separation: 8000 b (by TEM)

no. of jog traps / total traps $\lesssim 10^{-3}$

The unresolved (small) jogs can not be ruled out as being the sites for PA.

ICPA-7 (1982) 287

Y.H. Park et al.

P-N dislocation core model and positron annih. effects

位错中心 P-N 模型和正电子湮没效应

$$u_x = -\frac{b}{2\pi}\tan^{-1}\left(\frac{x}{\zeta}\right)$$

ζ, semi width of the disl. Simple 2-D model

ζ 是位错半宽度. =维的简化模型.

$$u_y = -(b/2\pi)\tan^{-1}\left(\frac{y}{\zeta}\right)$$

$$u_\theta = 0$$

位错中心的体积膨胀 volume expansion in the dislocation core

$$f(r) = \mathrm{div}\,\vec{u}$$

$$= -(b/2\pi r)\tan^{-1}\left(\frac{r}{\zeta}\right) - \frac{b}{2\pi\zeta}\,\frac{1}{1+(\frac{r}{\zeta})^2}$$

$\rho_c(r) = \rho_0[1+f(r)]$ (位错心处电子密度)

ion density in the disl. core

$$= \rho_0\left[1 - \frac{b}{2\pi r}\tan^{-1}\frac{r}{\zeta} - \frac{b}{2\pi\zeta}\,\frac{1}{1+(\frac{r}{\zeta})^2}\right]$$

$\Delta\tau = \tau_d - \tau_f = 13$ ps ; $E_b = 1.1$ ev

compare with binding energy due to vacancy

$E_b^v = 2.2$ ev Shen J.P. & Wang C.W. Wang K.L.

Proc. ICPA-7 (1982)

phys. stat. sol. (b) 134. (1986)

compare with Martin and Padanis results of disl. (1982)

$E_b^d \approx 0.1$ ev.

compare with Arponen et al. (1973)

$E_b^d = 2.79$ ev.

PA parameters in various models

Models	τ_b (ps)	τ_f (ps)	E_b (ev)	$\Delta\tau/E_b$ (ps/ev)
Vacancy	251	168	2·2	37·7
Cylindrical hole	229	168	2·1	29·0
Arponen et al.	229	168	2·8	21·8
P-N Model	183	168	1·1	13·6

The extended character of the defect model increases, $\Delta\tau/E_b$ value drops down.

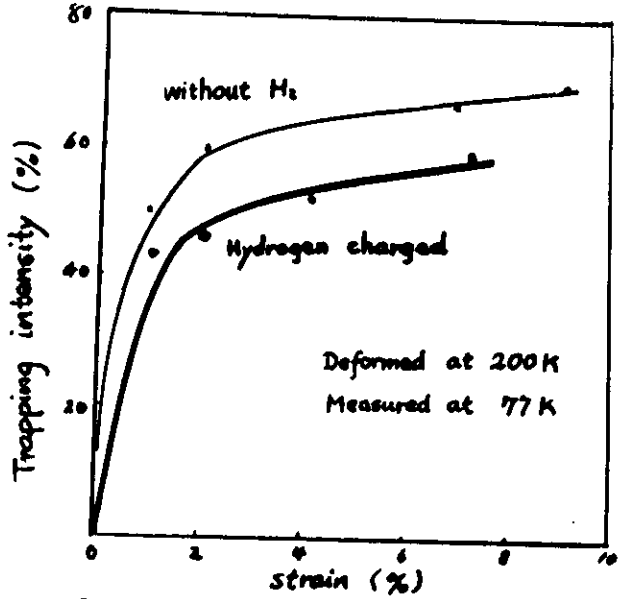

Fig. Fe single crystals deformed in tension at 200K

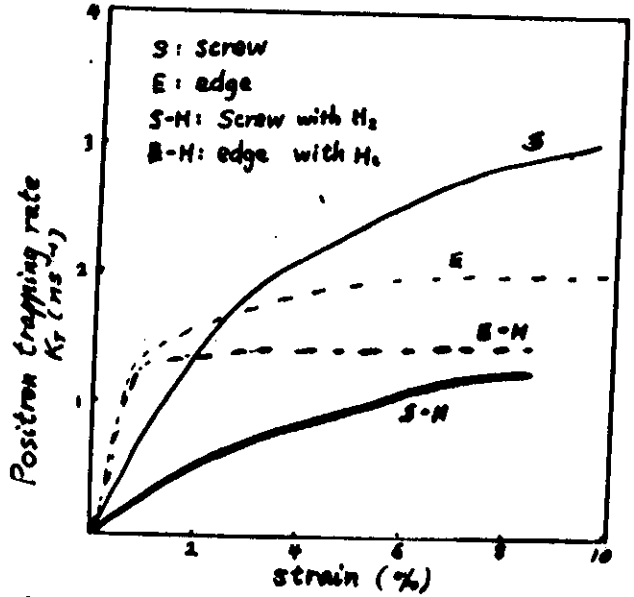

The H effect is larger in a screw dislocation than in an edge dislocation!

Proc. ICPA-7(1985)590
V.K. Paik et al.

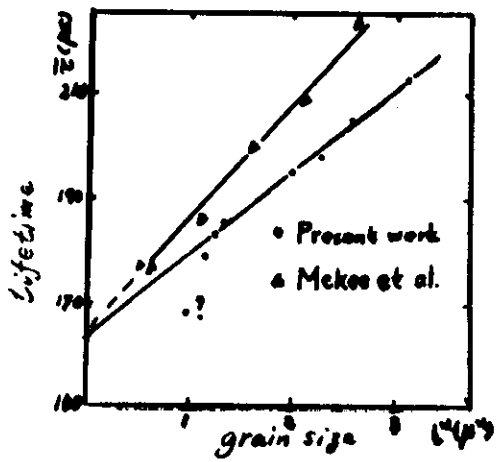

Heat treatments and measured results

No.	Temp. 热处理温度	Time 保温时间	quenching 冷却方法	grain size $\bar{l}$ (μm)	Lifetime $\bar{\tau}$ (ps)
6	380°C	0.5hr.	冰盐水淬	0.58	218
2	350°C 250°C	0.5hr.	冰盐水淬 空冷	0.39	205
1	350°C 250°C	0.5hr.	冰盐水淬	0.44	198
15	280°C	0.5hr.	炉冷	0.50	195
3	380°C 250°C	0.5hr.	冰盐水淬 水淬	0.76	186
14	250°C	0.5hr.	风冷	0.86	179
12	280°C	0.5hr.	油淬	1.02	168
16	试样原始态			0.80	183

(周先意、王淑荣、蒋建林、姜健、龙期威), 1984.
ZHOU, WANG, JIANG, JIANG, LUNG

裂缝顶端范性区的正电子湮灭

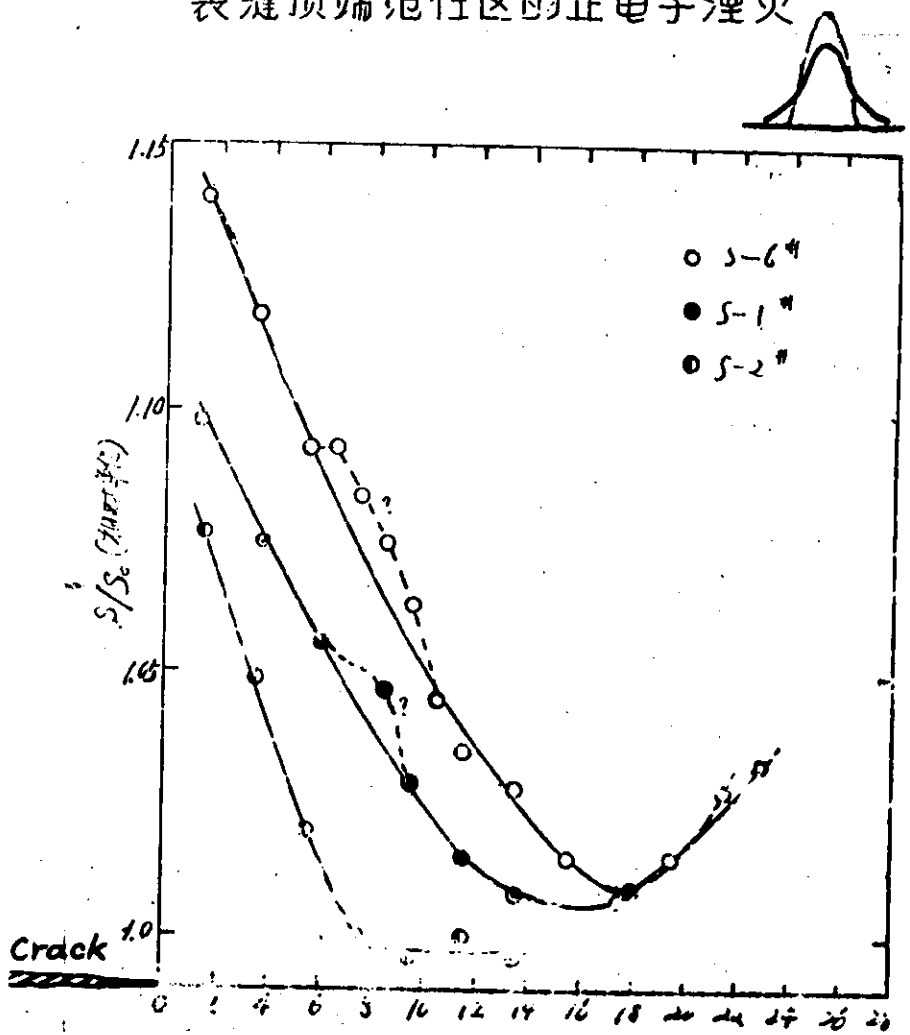

Positron annihilation in the plastic zone at a crack tip
in 《Positron Annihilation》, (1982) 481. 1981. c.
North-Holland Publ. (Jiang, Xiong, Lung et al.)

1, Dislocations and vacancies were mixed.
2. can not see DF2
3. can measure the plastic zone size*
* Xiao Jimei et al. Scripta Met. 16(8),

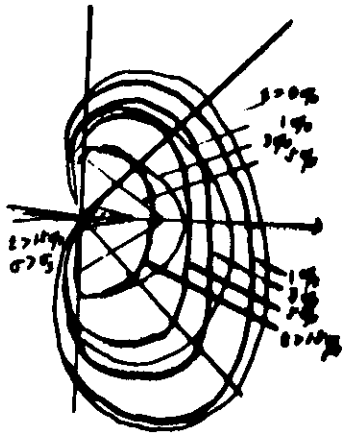

Fig. The H effects on the plastic zone of cracked 40MnMo steel measured by PA.

Tien Z. et al. Scripta Met., 16 (1982), 383

Fatique:

L. Dias, R. Pareja et al. Proc. ICPA-7 (1985) 579.

L. Dias, R. Pareja et al. Phil. Mag. A1, 6 (1985) L61.

S. J. Wang et al. Proc. ICPA-7 (1985) 467.

Wang et al: (Ni polycrystalline)

1. multi-exponential fitting method. (3)
2. τ_1^0 : e^+ free lifetime.
3. τ_{2A}, τ_{2B} 209-255 → 340 ps — logN (N: 10 → 10^6) vacancy clusters
4. τ_{1A}. τ_{1B} saturation value ~ 168 ps dislocation loop / vacancy
5. $\tau_3^0 = \tau_{2A}' = \tau_{3B}$ due to specimen surface.

Dias et al.

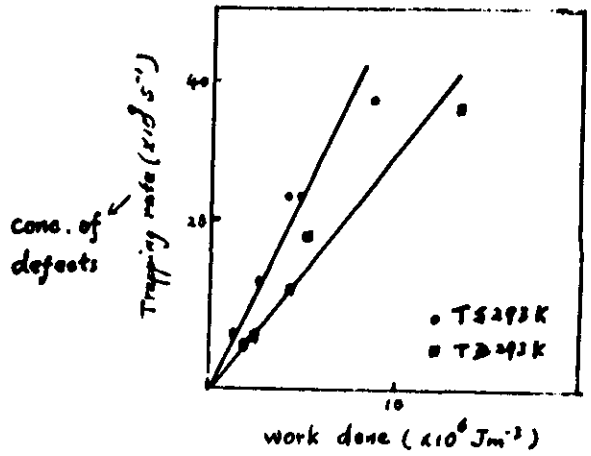

Nanocrystalline iron

[illegible] and R. Würschum, 1986
(Preprint)

[illegible] crystallites sizes: 5 - 10 nm (0.005 - 0.01 μm)

1. volume fraction of interfacial structure
   20 - 50 % (3 - 10 nm)

2. τ_1 is similar to the lifetime $\tau_{iv} = 175$ ps observed at monovacancies in bulk iron.

3. τ_1 persist up to temperature $T = 320°C$ (not recover below this temperature)

4. τ_2 is attributed to positron trapping at microvoids at the intersection of several crystalline interfaces. (τ_2 also persists up to temperature $T = 320°C$)

1. What are the limits ?

2. What are the merits and demerits ?

3. Where does PA stand in relation to other techniques ?

Pls refer.

« Positron Annihilation » Proc. ICPA-7.
1985, p. 437. (SMR/208 - 2)